Seismic behaviour of reinforced concrete interior beam-column connections with proposed reinforcement details

(Vandana RK, Bindhu KR)

Abstract

The present philosophy of earthquake resistant design is to ensure post elastic deformation without collapse of structures in case of severe earthquakes. Hence, special confining reinforcement are provided in columns and beams to promote ductile mode of failure of beam column joints. But this results in congestion of reinforcement at the joints. To reduce the reinforcement congestion at the joint region, three novel detailing patterns for reinforcement are proposed in this study. Seven interior beam column joint specimens were tested to failure under cyclic loading, and the effect of reinforcement detailing pattern on strength and ductility behaviour is meticulously examined.

.**Keywords**: rc interior beam column joints, cyclic loading, seismic behaviour, novel reinforcement detailing, plastic hinge relocation

The present philosophy of earthquake resistant design is to ensure sufficient post elastic deformation without collapse of structures in case of severe earthquakes. Critical zones in earthquake resistant structures must therefore have the required ductility to allow for this deformation. Hence besides strength, ductility requirements become essential for safety against brittle collapse without warning under excessive loads. In the limit analysis of multi storey frames it is assumed that sufficient number of plastic hinges is formed to transform either the whole or part of the structure into a mechanism. The rotation capacity of the hinges must be sufficient to permit full moment distribution. This ductile performance of the plastic hinges is therefore the essential requisite for the development of full ultimate strength of the structure in disaster prone.

Beam-column joint is a critical component in the design of moment-resisting frames as they are the weakest links in the structure. Joints with sufficient shear strength dissipate energy safely without causing any collateral damage. Ductile beam hinge mechanism is prevalent in such joint failures. World-wide, earthquake-resistant design codes promote joint ductility by incorporating the strong-column weak-beam mechanism. In this mechanism, the plastic hinges develop in beams at the beam-column interface while all vertical members remain elastic in order to provide maximum energy dissipation during an earthquake (Paulay & Priestley, 1992; Penelis & Kappos, 2010). In order to promote this behaviour in beam column joints, most of the internationally accepted building codes have provided guidelines regarding the detailing of reinforcement. ACI 352R-02 (2002), NZS 3101 (2006), ACI 318M-14 (2014) and IS 13920 (2016) have provisions for the diameter, spacing and amount of the longitudinal as well as the

transverse reinforcements. Special confining reinforcement are provided in columns and beams or wherever applicable with the purpose of developing beam hinging mechanism under seismic loading. Design recommendations stipulate to provide reinforcement cage with closely spaced transverse reinforcement in the critical zones. This is aimed to provide better confinement for the core concrete and thus impart the required ductility. But this results in congestion of reinforcement at the joints in real three-dimensional multi storey frames where three or more members will be meeting at the joints, leading to construction difficulties (Park & Ruitong, 1988). Studies on methods for improving ductility without increasing congestion, using non-conventional reinforcement detailing, have therefore got great significance (Au, Huang & Pam, 2005; Chalioris, Karayannis, & Favvata, 2007; Chalioris, Favvata, & Karayannis, 2008; Abbas, Mohsin, & Cotsovos, 2014).

Three types of joint failures are observed generally in earthquake prone areas. In the first category, joints fail in shear without affecting the strength of beams framing the columns. This type of failure is brittle and sudden; it must be avoided at any cost. In the second category, beams yield and fail without affecting column or joint safety. This is the preferable mode of failure in moment-resisting frames when under seismic loading. In the third category, joint failure occurs as a combination of beam yielding followed by joint shear failure (Goto & Joh, 1996; Shiohara & Kusuhara, 2009; Xing et al., 2013).

The study conducted by Paulay, Park & Priestley (1978) is a pioneering one, as it found that two postulated mechanisms such as strut and truss mechanisms are responsible for the shear resistance in a joint core. In the strut mechanism, joint shear is transferred via a diagonal concrete strut that sustains only compression. The truss mechanism considers the shear resistance contribution of vertical and horizontal reinforcement inside the joint core. The two mechanisms are superimposed to resist the total joint shear force in the horizontal and vertical directions.

Anchorage length of beam bars is reported (Leon, 1989, 1990) to be another influential factor in affecting the energy dissipation capacity of joints. As per these studies, an anchorage length of 28 times the bar diameter was necessary to ensure a weak-girder strong-column mechanism through a severe load history. There are contradictory reports on the effect of column axial load on the general behavior of joints. It has been reported that while increased axial loads are favorable to the energy dissipation capacity of joints with small shear, this may cause concrete crushing in joints with high shear (Pantazopoulou & Bonacci, 1992; Fu et al,. 2000). But Bakir & Boduroglu (2006) reported that the column axial load is one of the most influential factors on the bond performance of joints.

A finite element model developed by Pantazopoulou and Bonacci (1994) has been successful in assessing the parametric dependence of joints under lateral loads. Joint hoops were found to not only confine the joint

cores but also contribute in the shear resisting mechanism of the joint panel. It was also observed that participation of the joint core concrete in the mechanism of shear resistance is decreased as the number of joint hoops is increased.

Debonding of beam bars is found to be another important factor that affects the shear transfer mechanism. Kitayama, Otani, & Aoyama (1991) reported that to check the bond deterioration of beam bars, the ratio of column width to beam bar diameter is to be limited as a function of the beam bar strength and concrete strength.

Scaling-related effects have raised concerns over the reliability of testing on reduced-scale model structures. The study conducted by Abrams (1987) summarized tests of small-, medium-, and large-scale joints. It was reported that, although there were quantitative differences in behavior for specimens of different scales, the same resistance mechanisms were observed for all specimens. Even at one-twelfth scale, the physical models reflected hysteretic characteristics more similarly than most numerical models used in research and in practice. Since force-deflection behavior was simulated well using specimens constructed at one-quarter or larger scales, the study recommended that the minimum usable scale factor for testing isolated reinforced concrete components in flexure be one quarter. This conclusion was supported in another study conducted by Lu et al. (1999) in which the effect of using reinforced concrete scale columns under cyclic action was investigated. The test column specimens were constructed on three scales: 1:2, 1:3, and 1:5.5. All the specimens were reported to behave in a similar manner independent of their scale. In the present study, the specimens were constructed at one-third scale, making them more resistant to scaling-related effects.

Lack of basic data seems to be the stumbling block in assessing the contribution of various parameters towards the joint shear strength. The primary variables contributing the joint shear strength are observed to be the concrete strength, transverse reinforcement and presence of transverse beams and slabs (Meinheit & Jirsa, 1977; Bonacci & Pantazopoulou, 1993; Kim & La Fave, 2008). Transverse beams confine joints by means of their longitudinal reinforcement, which are anchored inside the joints in the transverse direction, as well as by effectively increasing the volume of joint concrete that actively participates in the joint's shear-resisting mechanism.

Some research studies proved that high concrete strength promotes joint shear strength and reduces the rate of stiffness degradation in a healthy way (Durrani & Wight, 1985; Alva et al., 2007; Vandana & Bindhu, 2017; Vandana, Bindhu, & Baiju, 2018). However, Meinheit & Jirsa, (1977) also showed that joint shear strength degradation occurs regardless of concrete strength. In the study conducted by Shohara (2004), it is suggested that the concrete compressive strength is not the primary factor promoting shear strength. Increase in shear strength occurs because of the influence of the bond capacity of longitudinal reinforcement,

which in turn is assumed to be proportional to the square root of concrete compressive strength. The axial force level of the column due to the confining effect or transverse beams covering a joint, concrete cover thickness, diameter and number of bars, reinforcement yielding, and cyclic loading were reported as the major parameters influencing the bond capacity.

Another significant factor influencing the joint shear strength is the aspect ratio, defined as the ratio of beam depth to column depth. It is reported that higher aspect ratios result in lowering the shear strengths of interior and exterior beam-column joints (Shiohara, 2004; Mitra & Lowes, 2011).

In the study conducted by Shen et al. (2021), a novel reinforcement detail consisting of diagonal bars mechanically anchored at beams are proposed for beam-column joints. The results exhibited improved seismic behaviour and the plastic hinges formed were away from the joint core.

Systematic variation of every parameter affecting shear strength is beyond the scope of any realistic experimental study. However, selecting certain parameters and varying them can provide important insights into joint shear behavior. Very Limited studies have considered the effect of reinforcement detail on shear strength of joints. This aspect needed to be thoroughly investigated. Aspect ratio is another variable whose effect on joint resistance has not yet been explored in detail. Various tests have provided contradictory views on the effect of concrete compressive strength on joint shear behavior; however, its effect on the ductile behavior of joints has not been investigated thoroughly.

The scope of the present study is to compare the behaviour of beam column joint specimens using different joint reinforcement detailing experimentally. Three new detailing patterns for reinforcement at joint region are proposed in this study. In the first two cases, the proposed non-conventional reinforcement is provided in the form of diagonal reinforcement on the faces of the joint as a replacement of ties in the joint region. In the third case, the newly proposed reinforcement is provided in the form of diagonal collar stirrups instead of rectangular ties in the joint region. These proposed reinforcement detailing have the basic advantage of reducing the reinforcement congestion at the joint region. The effect of reinforcement detailing pattern on strength and ductility behaviour is meticulously examined. In addition to this, the effects of design characteristics like concrete compressive strength, aspect ratio and area of column longitudinal reinforcement in combination with the best proficient detailing pattern are also investigated.

Experimental

Experimental investigation consisted of testing twelve interior beam column joint specimens with proposed detailing pattrn to analyse the seismic behaviour. The detailing pattern which exhibited the best seismic resistance is recommended as a suitable alternative to the conventional reinforcement detailing currently being used in practice. The concrete mix design is conducted as per the guidelines specified in IS 10262 (2009).

Proposed detailing patterns

A set of diagonal ties are designed in such a way that the total volume of ties in the joint region remains the same as the volume of rectangular ties in the joint region of a specimen detailed as per IS 13920 (2016). Detailing pattern of a pair of bars resembles letter 'X' in the joint region and the ends of these bars extend to a length equal to at least the development length into the column or beam. These cross inclined bars are used as alternative ties at the joint region. Out of the three proposed detailing patterns, the first one is a pair of bars of X-type confining reinforcement placed in alignment with the beam axis. In the second case, X-type confining reinforcement consisting of 2 diagonal bars is placed in alignment with the column axis. In the third case, the proposed confining reinforcement in the form of diagonal ties or collar stirrups in the joint region of the specimen are incorporated in the joint.

Specimen characteristics

All test specimens have common overall length measured 1300 mm for columns and 1500 mm for beams as well as common column cross-sectional area of 150 mm × 100 mm. The beam column joint test specimens are designated as CTRL, SXB, SXC, SXJ, SXJ35, SXJI, and SXJ8. The specimen CTRL conforms to the conventional reinforcement detailing intended to be seismic resistant as per IS 13920 (2016). The specimen SXB has the same longitudinal reinforcement as CTRL but the joint transverse reinforcement is replaced with the X type confining reinforcement aligned along the beam axis. The specimen SXC has the same configuration as that of SXB except that the X-type confining reinforcement within the joint region is aligned along the column axis. The specimen SXJ is designed with the third proposed reinforcement detailing in which diagonal ties or collar stirrups are used at the joint panel region. All the other characteristics of SXJ are same as that of specimen CTRL. The specimens SXJ35, SXJI, and SXJ8 have same reinforcement configuration as that of SXJ, but different geometric and material characteristics as listed in Table 1. The specimen SXJ35 is cast with M35 grade concrete with the intention of assessing the combined effect of concrete compressive strength and the collar stirrups on joint seismic behaviour. The specimen SXJI is designed with an aspect ratio of 0.67 with the intention of quantifying the detrimental effect of aspect ratio when used in combination with diagonal ties. In the specimen SXJ8, 8mm longitudinal bars are used in column instead of 6mm bars as in other specimens. This change in diameter of reinforcement has increased the area of column longitudinal reinforcement by 77 percent. The diameters of X type bars, collar stirrups, transverse reinforcement and beam longitudinal bars are kept as 6mm. The reinforcement detailing patterns and specimen dimensions are represented in Figures 1. to 4.

Materials used

Ordinary Portland cement (53 grade), M-sand passing through a 4.75 mm IS sieve (fineness modulus, 2.5; specific gravity, 2.5) and crushed stone of maximum size 12 mm (specific gravity, 2.76) and size 6 mm (specific gravity, 2.74) were used for this investigation. The bars of

diameter 6 mm and 8 mm having specified yield strengths 500 MPa were used as reinforcement. The mechanical properties of high yield strength deformed (HYSD) bars used for preparing the specimens were tested (IS1786 2008; IS 1599 2012) and are tabulated in Table 2. The reinforcement strain during testing is measured by means of electrical resistance strain gauges (resistance, 350 Ω; gauge length, 10mm) fixed on the beam longitudinal bars at the beam column interface.

Test procedure and instrumentation

The specimens are supported in vertical position in a steel loading frame of capacity 2000 kN. An axial load of 10 percent of the column axial capacity is applied at the top of the column with a hydraulic jack (capacity, 250 kN), thus ensuring adequate stiffness capacity as well as providing moments at the joint. The beam ends are subjected to reverse cyclic loading

Table 1. Geometric and material characteristics of specimens

Designation of Specimens		*CTRL*	*SXB*	*SXC*	*SXJ*	*SXJ35*	*SXJI*	*SXJ8*
Aspect ratio (A_{spr})		*1*	*1*	*1*	*1*	*1*	*0.67*	*1*
Yield strength of longitudinal bars (MPa)	*Beam*	*500*	*500*	*500*	*500*	*500*	*500*	*500*
	Column	*500*	*500*	*500*	*500*	*500*	*500*	*500*
Cross section (mm^2)	*Column*	*150×100*						
	Beam	*100×150*					*100×100*	*100×150*
Reinforcement diameter in column (mm)	*main bars*	*6*	*6*	*6*	*6*	*6*	*6*	*8*
	stirrups	*6*	*6*	*6*	*6*	*6*	*6*	*6*
Reinforcement diameter in beam (mm)	*main bars*	*6*	*6*	*6*	*6*	*6*	*6*	*6*
	stirrups	*6*	*6*	*6*	*6*	*6*	*6*	*6*
Designation of concrete mix		*M30**	*M30*	*M30*	*M30*	*M35*	*M30*	*M30*
Average f_{ck} †(MPa)		*40.71*	*37.62*	*38.51*	*39.2*	*44.67*	*39.56*	*39.02*
Average f_c' ‡(MPa)		*33.29*	*32.15*	*32.87*	*33.46*	*39.86*	*33.52*	*32.98*

* M refers to the mix and the number to the specified compressive strength of 150 mm size cube at 28 days in N/mm^2

† Concrete cube compressive strength on the day of testing

‡ Concrete cylinder compressive strength on the day of testing

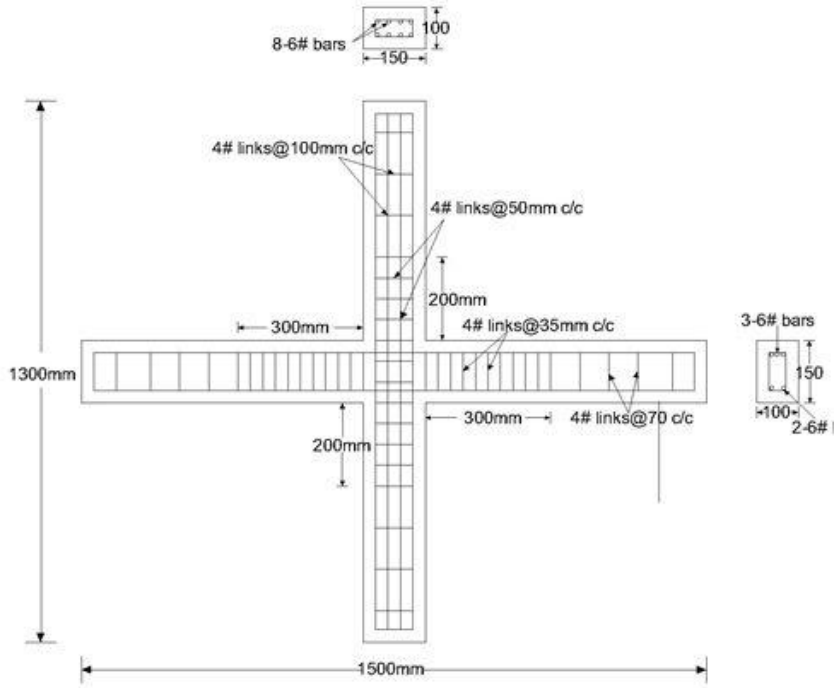

Fig. 1 Detailing of conventional specimen CTRL

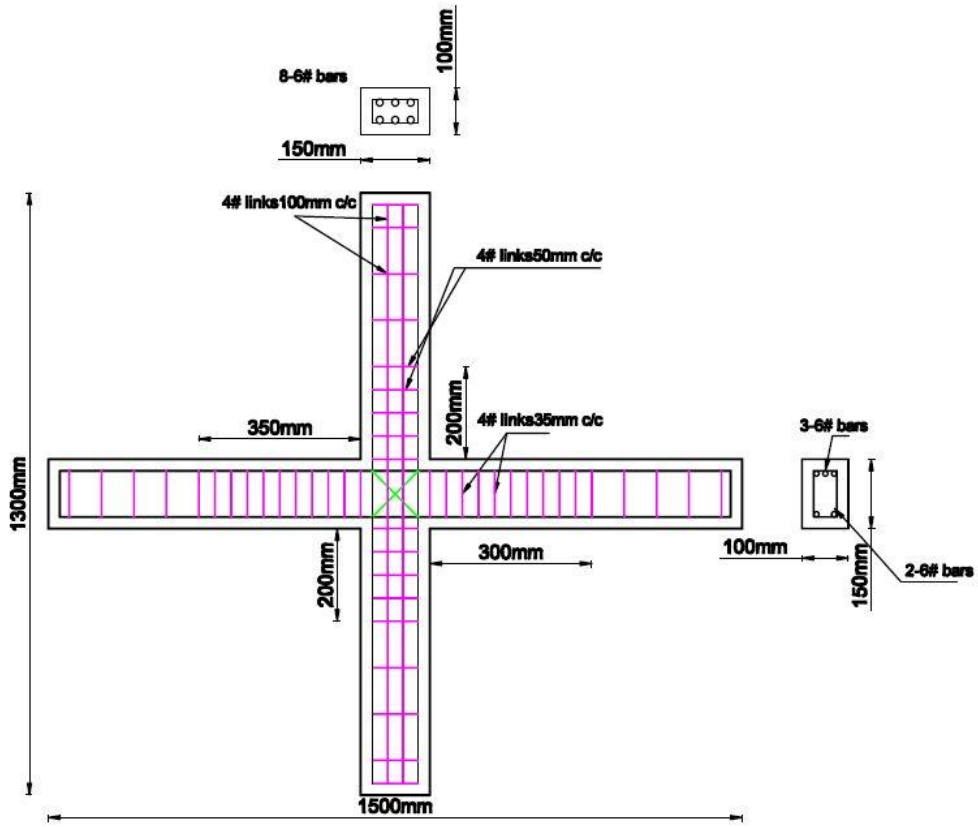

Fig. 2 Detailing of specimen SXJ

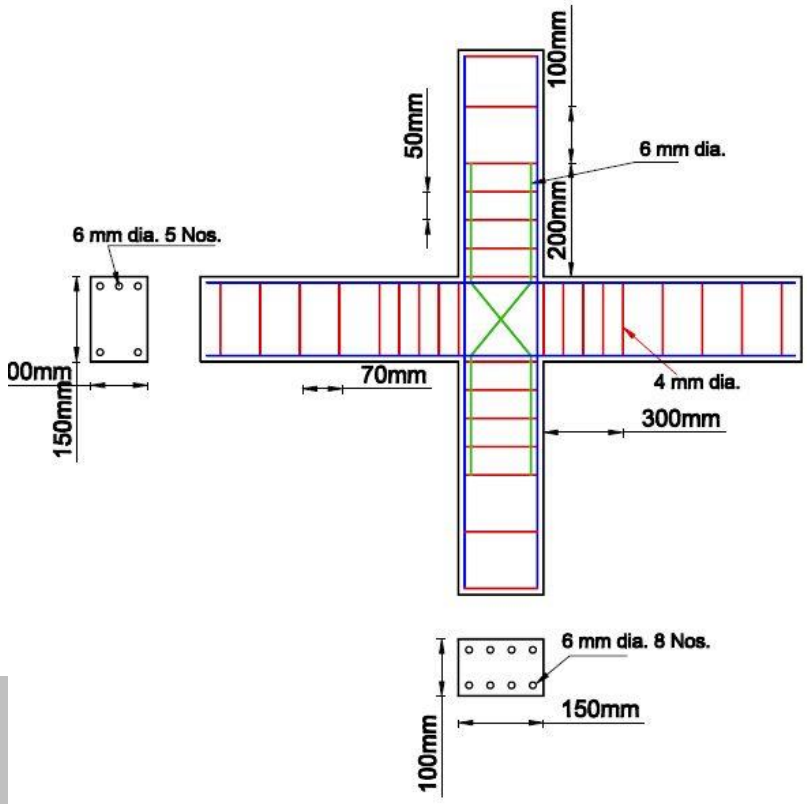

Fig. 3 Detailing of specimen SXC

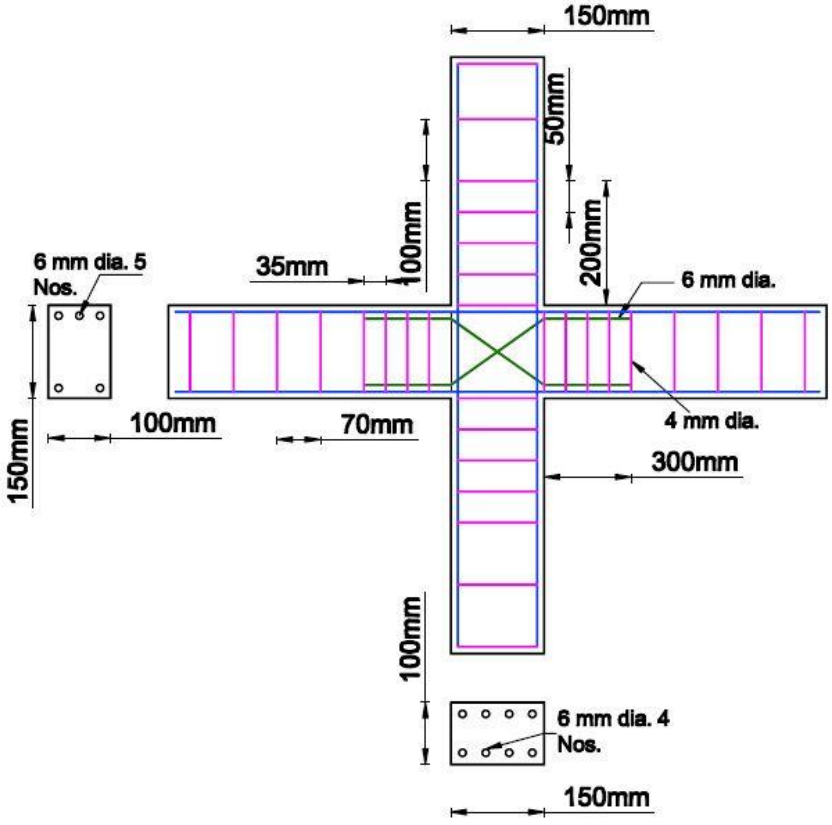

Fig. 4 Detailing of specimen SXB

Table 2. Properties of High yield strength deformed bars

Diameter (mm)	*Specified yield strength* (MPa)	*Actual yield strength* f_{ya} (MPa)	*Ultimate tensile strength* f_{tu} (MPa)	f_{tu}/f_{ya}	*Percent elongation*	*Modulus of elasticity* (MPa)	*Bending Strength* (MPa)
6	*500*	*514.60*	*617.40*	*1.20*	*17.50*	1.99×10^5	*620*
8	*500*	*516.55*	*620.05*	*1.20*	*16.40*	1.95×10^5	*635*

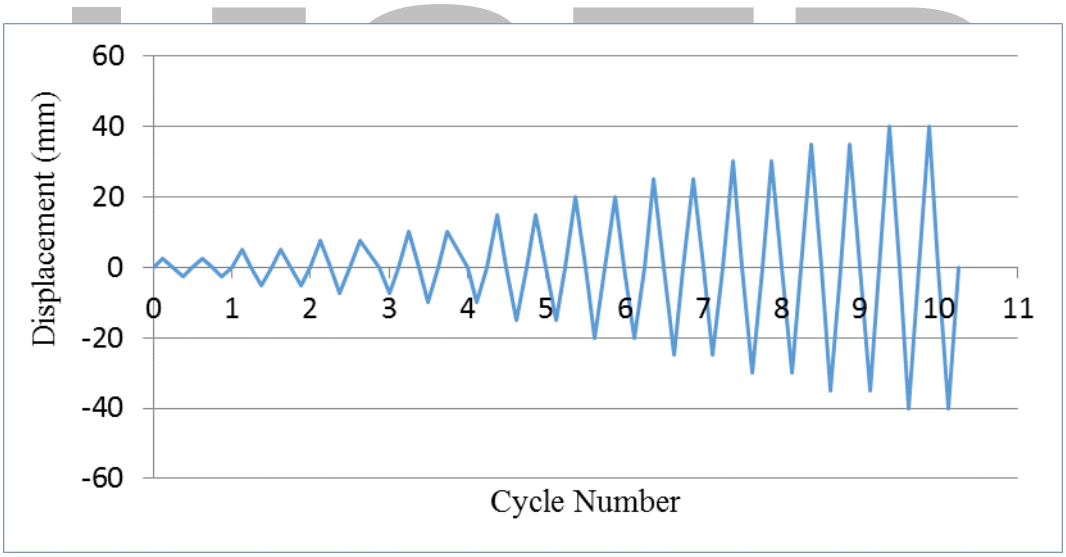

Fig. 5 History of cyclic loading applied at the beam ends

with screw jacks (capacity, 250 kN). By reversing the direction of the lateral loads applied at the beam ends, the earthquake type loading is simulated (Meinheit & Jirsa, 1981). The reactive shear at the ends of the column is induced by the applied lateral loads at the beam ends. For all the tests on the interior beam column joint units, similar loading history is used. Gradually increasing reverse cyclic displacement is applied laterally at the beam ends with the displacement increment of 2.5 mm (δ_1, $2\delta_1$, $3\delta_1$, *etc*.). Beyond the yield strength of longitudinal beam bars, the displacement increment is changed to $2\delta_y$, $3\delta_y$, *etc*. (where δ_y is the displacement when yielding starts), until failure. The specimens are loaded up to a certain magnitude of displacement and then unloaded in the opposite direction and reloaded in order to obtain a full cycle of reverse loading.

Each loading cycle is repeated twice; after each cycle, the magnitude of displacement is increased. The process is continued until the specimen reached its maximum capacity. Thereafter, the loading is applied without repetition of the loading cycle until failure (Kitayama, Otani, & Aoyama, 1988; Stevens, Uzumeri, & Collins, 1991; Park & Milburn, 1998; Shin & LaFave 2004; Li, Mander, & Dhakal, 2008). Figure 5 represents the cyclic loading history. In each loading stage, the deflection at the tips of the beams are measured using two linear variable displacement transducers (LVDTs) having a least count of 0.01 mm and gauge length of 200 mm. The strain in the beam longitudinal bars is measured using the strain gauges installed in each beam column joint specimen. The strain, deflection and load cell readings are recorded using a data acquisition system (National Instruments, DAQ SCXI series). Figures 6 (a)-(b) represent the photograph and schematic diagram of the test setup in the laboratory used for the present study. Figure 5 represents the cyclic loading history. In each loading stage, the deflection at the tips of the beams are measured using two linear variable displacement transducers (LVDTs) having a least count of 0.01 mm and gauge length of 200 mm. The strain in the beam longitudinal bars is measured using the strain gauges installed in each beam column joint specimen. The strain, deflection and load cell readings are recorded using a data acquisition system (National Instruments, DAQ SCXI series). Figures 6 (a)-(b) represent the photograph and schematic diagram of the test setup in the laboratory used for the present study.

Behavior of test specimens

The behavior of the specimens are discussed by classifying them into two groups. The control specimen CTRL and specimens SXJ, SXC and SXB are included in the first group where the only variable is reinforcement detailing pattern. These specimens are designed with unit aspect ratio and M30 concrete strength. The reinforcement used in column and beam are of Fe 500 grade and of 6mm diameter. The specimens SXJ, SXJ35, SXJI and SXJ8 constitute the second group of specimens. These specimens have same reinforcement detailing, but have different geometric or material properties. In the case of specimen SXJ35, the concrete mix used is of grade M35. All the other details are same as that of specimen SXJ. The specimen SXJI is designed with an aspect ratio of 0.67. In specimen SXJ8, 8 mm bars are used as column reinforcement while in all the other specimens in the group, the bars used are of 6 mm diameter.

The general behavior of the test specimens is identified on the basis of the failure modes, visible crack patterns, hysteresis responses, strength and deformation behaviour, stiffness and reinforcement strains.

Mode of failure

Three different types of failure have been observed in test specimens under reverse cyclic loading. The specimens SXJ, SXJ8, SXJ35, SXJI and SXC have experienced beam flexural failure (BF) while the specimen SXB failed in joint shear (JF). The mode of failure of CTRL

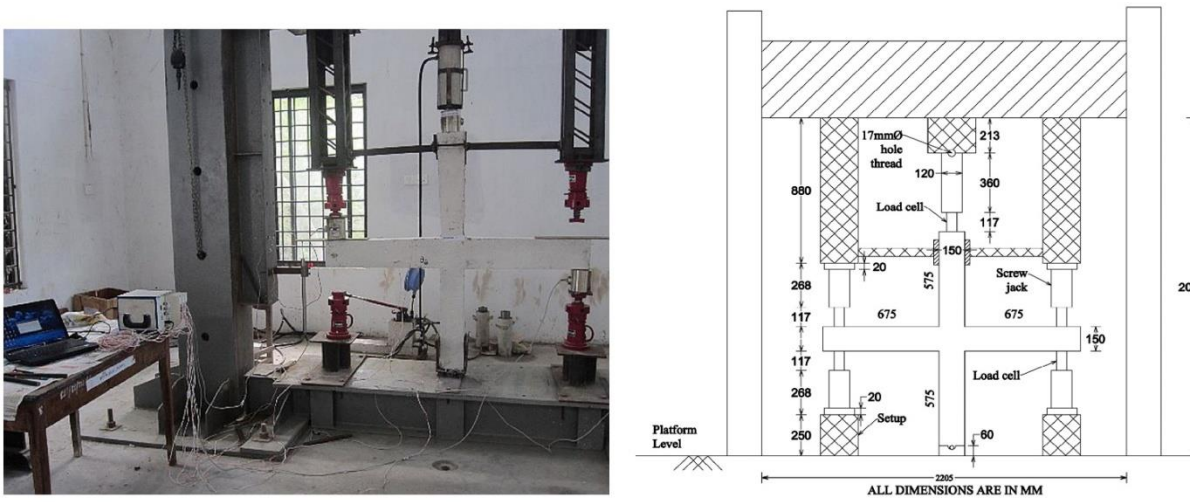

(a) Test setup

(b) Schematic Diagram

Fig. 6 Test setup

specimen is observed to be a combination of beam failure and joint shear failure (BJF).

Crack patterns

In specimen CTRL, first crack is observed at the junction between the beam and the column. As the rate of loading increased, the initial cracks widened and additional cracks are formed in the beam and joint panel. In specimen SXJ where the diagonal ties are used, the first crack is observed in beam at the beam column interface. With the increase of loading, more cracks developed in the beam than in the joint region. Cracks at the beam column interface widened with loading and finally the specimen failed in beam flexure. The initial cracks in specimen SXC occurred in beams and beam column interface. The cracks spread across the joint panel as the loading increased. The number of cracks appeared in the joint panel of SXC is relatively less compared to that in the beam. The initial cracks in specimen SXB are developed in the joint panel. The cracks spread across the joint region with some cracks in the column members and a few cracks in the beam, indicating the distribution of shear stresses over the joint and frame members; finally the specimen failed in joint shear. The initial cracks observed in specimen SXJ35 appeared in beams. The cracks later spread across the joints. The cracks in the beam are widened as the loading increased. The specimen ultimately failed in beam yielding. The specimen SXJI with an aspect ratio of 0.67 is observed to exhibit a beam failure. The first crack is observed in the beam column interface. Further increase in loading resulted in the development of additional cracks in the beams and joint panels. The initial cracks in specimen SXJ8 is observed to be similar in appearance to that of specimen SXJ35.The initial cracks appeared in beams and the cracks later spread across the joints. The cracks in the beam are widened as the loading increased. The width of

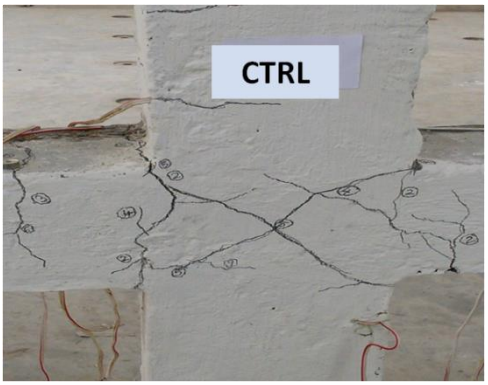

(a) Specimen CTRL

(b) Specimens SXC and SXB

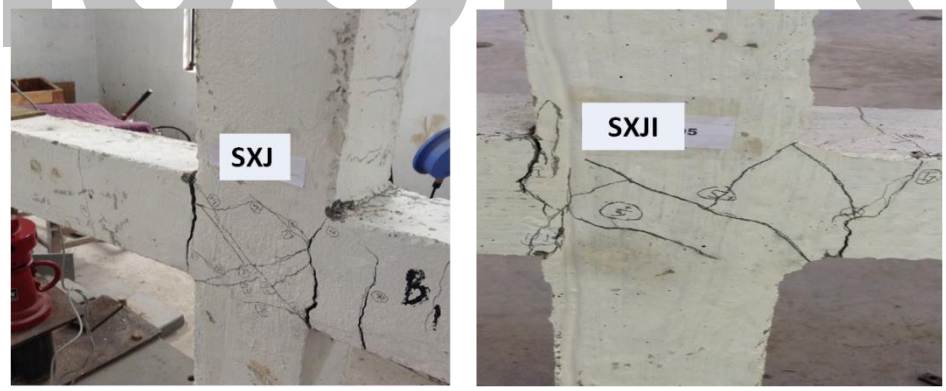

(c) Specimens SXJ and SXJI

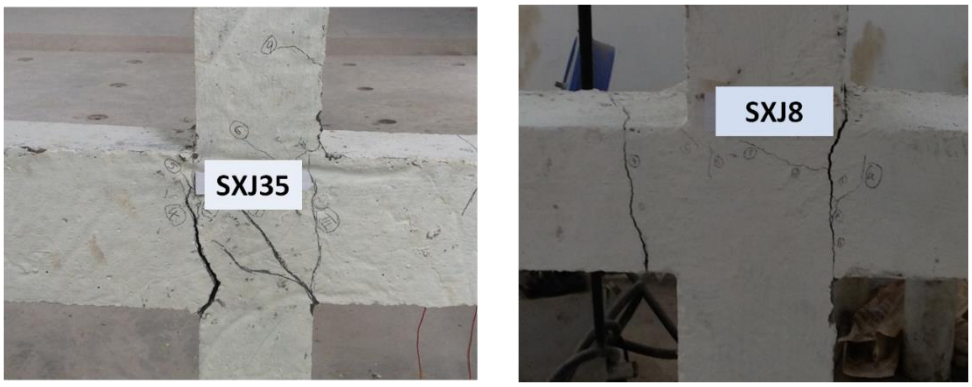

(d) Specimens SXJ35 and SXJ8

Fig. 7 Crack pattern of test specimens

cracks in beams of specimen SXJ8 are observed to be larger compared to that of specimen SXJ35. The specimen SXJ8 has failed in beam yielding. Figures 7 (a)-(d) represent the modes of failure of different specimens.

Hysteresis behaviour

The hysteretic response of the joint specimens is recorded throughout the loading cycle, as shown in Figures 8(a)-(g). The thick line at the center of the graph represents the initial cycles of loading until the specimens started to yield. The wider loops are those that were obtained after reaching the elastic stage. Each loading cycle is repeated twice; the curves may fall in the same path or have a gap between them. The gaps between the curves signify sufficient strength after crack occurrence. A single loading cycle is applied once the specimens reached the ultimate strength. The gaps between the hysteretic curves, which were obtained after reaching the ultimate load, are found to be wider, indicating strength degradation (similar to observation of Lu et al., 2012). The area of the hysteresis loops represents the energy dissipation capacity of each specimen. For clear comparison, the envelopes of the hysteresis loops of all the specimens are plotted in a single graph as shown in Figure 9.

Specimens CTRL, SXJ, SXC and SXB

The hysteresis loops of specimen CTRL is observed to follow a gradual and steady reduction in strength. The specimen sustained the load gradually through deformation until failure, as indicated by the wider gaps between the loops. The hysteretic curves indicate that even after reaching its ultimate strength, the specimen possessed sufficient strength for the two succeeding loading cycles.

The hysteresis loops of the specimen SXJ are steadier and more gradual than the hysteresis loops of CTRL specimen. The curves are very smooth and steady indicating the gradual attainment of maximum strength and later the gradual strength reduction. The area enclosed by the hysteretic loops of specimen SXJ is observed to be higher than that of specimen CTRL, indicating higher energy dissipation.

The hysteresis loops of specimen SXC are gradual but not steady. The gaps between the loops are comparatively smaller. The post failure cycles are observed to be limited in number. The area enclosed by the hysteretic loops appeared to be greater than that of specimen CTRL and lesser than that of specimen SXJ.

In the case of specimen SXB, the loops are observed to be closer, indicating poor shear performance. The curves are not close to each other for each displacement under two loading cycles. The specimen is observed to possess insufficient strength to complete at least one post failure load cycle. This indicates rapid strength reduction of the specimen under increasing load. The specimen failed in brittle shear failure ultimately.

Specimens SXJ, SXJ35, SXJI and SXJ8

In the case of specimen SXJ35, the hysteretic loops are steady and gradual till maximum load, indicating a gradual attainment of strength. But this performance is seemed to be inferior compared to the behavior of hysteretic

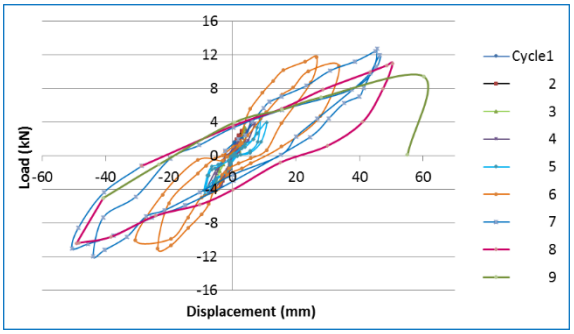

(a) Specimen CTRL

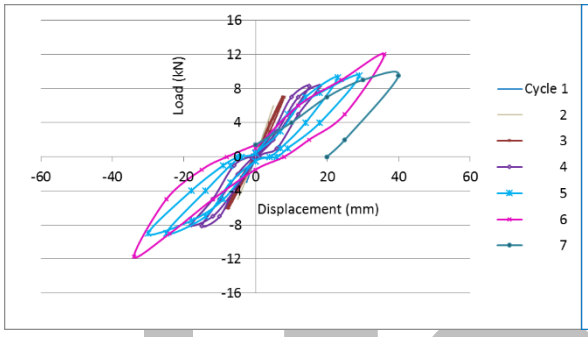

(b) Specimen SXB

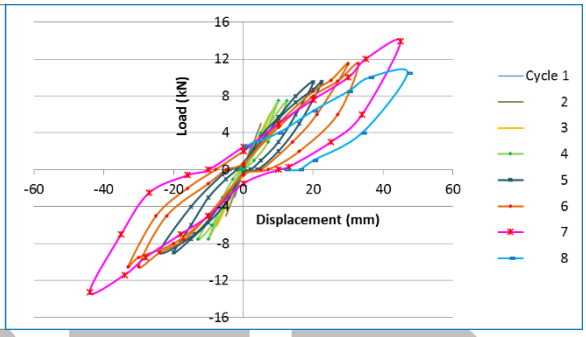

(c) Specimen SXC

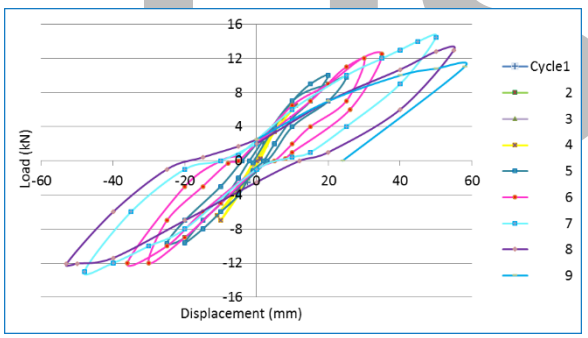

(d) Specimen SXJ

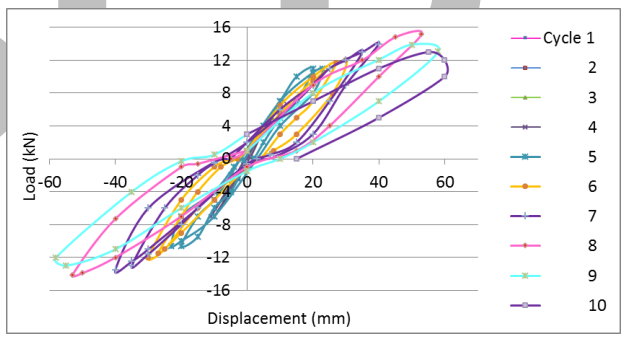

(e) Specimen SXJ8

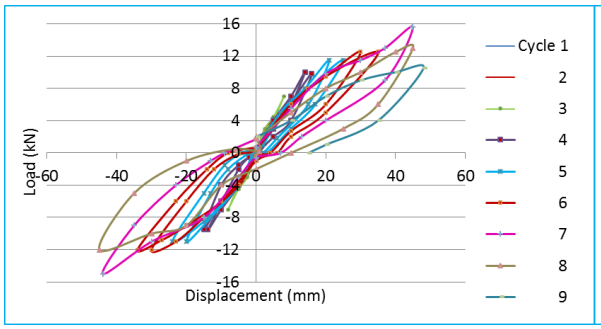

(f) Specimen SXJ35

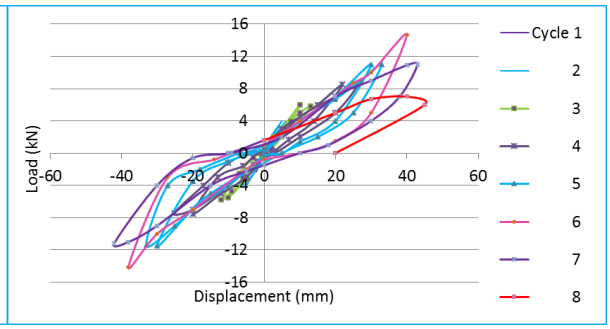

(g) Specimen SXJI

Fig. 8 Hysteresis loops of specimens

loops of specimen SXJ and the strength degradation occurred at a much faster rate.

The hysteretic loops of specimen SXJI appeared to be steep and altogether represent poor energy dissipation capacity and faster strength degradation. The closer loops indicate steady but rapid reduction in strength until failure. Ultimate load of SXJI is observed to be higher than that of specimen SXJ.

The hysteresis loops of the specimen SXJ8 are observed to be steadier and more gradual than the hysteresis loops of specimen SXJ. The curves are very smooth and steady indicating the gradual attainment of maximum strength and later the gradual strength degradation. The area enclosed by the specimen SXJ8 is observed to be higher than that enclosed by the specimen SXJ, indicating higher energy dissipation.

Ultimate load behavior of test specimens

The load and deformation values obtained during the testing of the specimens are tabulated in Table 3.

Specimens CTRL, SXJ, SXC and SXB

The ultimate load of the specimen CTRL is observed to be 12.75 kN. The ultimate load of specimen SXJ is obtained as 14.5 kN. The specimen SXJ exhibited an increase of 14 percent in ultimate load over that of CTRL. All specimens except SXB followed this pattern of load increase over CTRL. The provision of X type reinforcement along the column axis has helped in improving the ultimate load by 9 percent in specimen SXC. But the specimen SXB has been observed to exhibit a very poor performance concerning the ultimate strength. The ultimate load is found to decrease by 6 percent when X type reinforcement is positioned along the direction of beam in SXB. The specimen with proposed reinforcement detailing of collar stirrups at the joint is observed to withstand the highest ultimate load under cyclic loading.

Specimens SXJ, SXJ8, SXJ35, and SXJI

The ultimate load of the specimen SXJ is found to be 14.5 kN. The ultimate loads of SXJ8 and SXJ35 are increased by 5and 9 percents respectively while that of SXJI has not shown any noticeable increase compared to the specimen SXJ. The increase in ultimate load observed in the case of SXJI is only 2 percent. The maximum increase has been observed to occur for specimen SXJ35, indicating the significance of compressive strength in promoting the ultimate strength. The increase in joint strength was evident in the ultimate load exhibited by the specimen SXJ8. The variable which is most effective in improving the ultimate load when used in combination with the diagonal ties is observed to be the concrete compressive strength.

Joint shear behaviour

The observed joint shear strength of the test specimens are tabulated in Table 4. The reinforcement detailing pattern, aspect ratio and concrete compressive strength are observed to influence the joint shear strength significantly. The proposed reinforcement detailing pattern consisting of collar stirrups is found to be the most favorable approach in enhancing the shear strength of beam column joints under lateral loading.

Specimens CTRL, SXJ, SXC and SXB

The joint shear strength of

Table 3. Details of Load and deflection values of specimens

Specimen		*CTRL*	*SXB*	*SXC*	*SXJ*	*SXJ35*	*SXJI*	*SXJ8*
Yield Load (kN)	*Forward cycle*	*10.20*	*9.6*	*11.12*	*11.6*	*12.32*	*11.76*	*12.0*
	Reverse cycle	*9.53*	*9.2*	*10.64*	*10.4*	*11.6*	*10.80*	*11.12*
Deflection Corresponding to yield load (mm)	*Forward cycle*	*20.01*	*25.37*	*17.4*	*17.5*	*16.5*	*28.5*	*16.54*
	Reverse cycle	*19.50*	*24.30*	*16.95*	*16.80*	*16.10*	*27.90*	*15.85*
Ultimate load (kN)	*Forward cycle*	*12.75*	*12*	*13.9*	*14.5*	*15.4*	*14.7*	*15.0*
	Reverse cycle	*11.91*	*11.5*	*13.3*	*13*	*14.5*	*13.5*	*13.9*
Deflection Corresponding to ultimate load (mm)	*Forward cycle*	*45.50*	*36*	*40*	*50*	*45*	*40*	*53*
	Reverse cycle	*43.87*	*34*	*39*	*48*	*44*	*38*	*53*

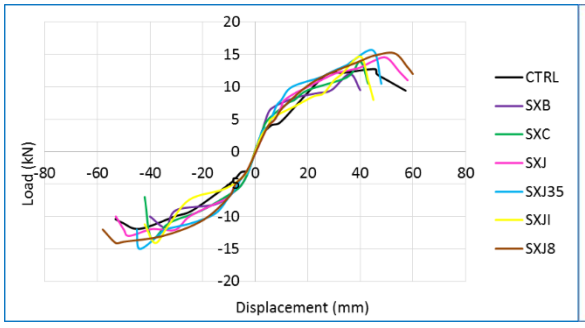

Fig. 9 Load-displacement envelopes

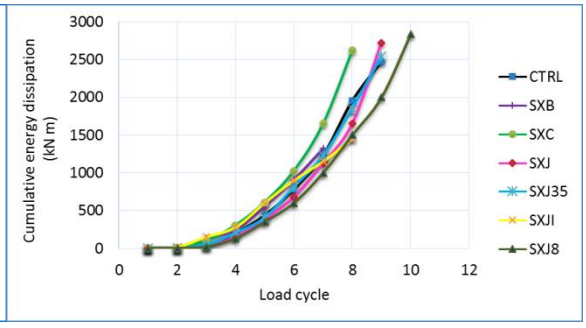

Fig. 10 Cumulative Energy Dissipation

specimen CTRL is observed to be 7.23 MPa. In the case of specimen SXJ, shear strength has been found to increase by 11 percent. The new detailing pattern involving diagonal ties at the joint region has been successful in resisting the shear effectively than the conventionally detailed specimen. In the case of specimen SXC, this increase is observed to be 10 percent, indicating a better reinforcement detailing as far as joint shear strength is concerned. The shear strength of the specimen SXB has been found to deteriorate by 5 percent. It is observed that out of the three reinforcement detailing patterns proposed, the provision of collar stirrups at the joint region and X type reinforcement along the column axis are better choices than the conventional detailing pattern as far as the shear strength of the joint is concerned.

Specimens SXJ, SXJ8, SXJ35 and SXJI

The shear strength of the specimen SXJ is calculated as 8.06 MPa. The shear strengths of the specimens SXJ8 and SXJ35 are observed to be increased by 5 percent and 9 percent respectively. The column reinforcement area and compressive strengths are found to influence the shear strength considerably. The specimen SXJI exhibited only 2 percent increase in its shear strength. The most significant variable in combination with the provision of diagonal ties in promoting shear is undoubtedly the concrete compressive strength.

Displacement ductility

The ductility of a structure is defined as its ability to undergo a large amount of deformation beyond the initial yield deformation while maintaining its strength. Displacement ductility is considered as a very important measure of seismic resistance of a structural component. The load-displacement envelopes of the specimens are plotted (Figure 9.) and the ductility factors are calculated accordingly (Shannag, Abu-Dyya, & Abu-Farsakh 2005). Table 4 represents the ductility values calculated for all the specimens. The ductility values are observed to be considerably enhanced in specimens designed with collar stirrups in the joint core.

Specimens CTRL, SXJ, SXC and SXB

In this group of specimens, SXJ exhibited the highest ductility factor of 3.08. Specimen SXB was observed to be the least ductile specimen, with a ductility factor of 1.45. The specimens SXC and CTRL have comparable ductility values of 2.71 and 2.61 respectively. The effect of proposed reinforcement detailing in SXB on joint ductility is observed to be very detrimental in nature. Similarly, the provision of X type bars aligned along the column axis is also not observed to produce any significant change in the ductility behaviour. The provision of diagonal ties at the joint region is found to be an excellent choice as it enhances the ductility values considerably.

Specimens SXJ, SXJ8, SXJ35 and SXJI

Among the specimens detailed with diagonal ties at the joint, SXJ8 exhibited the highest ductility factor of 3.33. The second best is exhibited by SXJ with a ductility factor of 3.08. The ductile behavior of SXJ35 is comparatively

good with a ductility factor of 2.65. The ductility value of the specimen SXJI is observed to be 1.48, indicating a very poor ductile performance compared to the rest of the specimens. The influence of unit joint aspect ratio in sustaining sufficient joint flexibility is very significant. This is evident in the difference in ductility values exhibited by the specimens SXJ and SXJI. The increase in area of column longitudinal reinforcement in combination with the diagonal ties at the joint region is observed to have the strongest influence on ductility of joints.

Energy dissipation capacity

The energy dissipation capacity is a direct measure of seismic resistance of the structural components. The area enclosed by the load-displacement hysteresis loop represents the dissipated energy during every load cycle (Leon, 1989; Shiohara, 2004; Mitra & Lowes, 2011). The cumulative energy dissipation curves of all the specimens are represented in Figure 10.

Specimens CTRL, SXJ, SXC and SXB

The energy dissipation capacity exhibited by the control specimen CTRL is observed to be 2.48 kNm. The energy dissipation capacities of specimens SXJ and SXC are found to be increased by 10 percent and 5 percent respectively. The lowest energy dissipation capacity is exhibited by the specimen SXB and the percentage decrease is found to be 47 % compared to that of specimen CTRL. The results indicate that the provision of X type reinforcement along the beam axis influence the energy dissipation capacity of joints negatively. The X type reinforcement along the column axis has not produced any significant effect on energy dissipation capacity. The provision of diagonal ties at the joint region is found to be a very fine alternative to the conventional reinforcement detailing in improving the energy dissipation capacity.

Specimens SXJ, SXJ8, SXJ35 and SXJI

The energy dissipation capacity of SXJ is taken as the basis for comparison among these specimens. The specimen SXJ8 exhibited highest energy dissipation capacity with an increase of 3 % over that of specimen SXJ. The highest compressive strength in the case of specimen SXJ35 has not been observed to produce any effect on energy dissipation capacity. This is evident in the 7 % decrease shown compared to that of specimen SXJ. Concrete compressive strength has not been observed to be a key player in enhancing the energy dissipation capacity of specimens detailed with diagonal ties in the joint region. The performance of specimen SXJI has demonstrated the power of unit aspect ratio in influencing the energy dissipation capacity. The energy dissipation capacity of the specimen SXJI is observed to decrease by 51 %. Increase in area of column longitudinal reinforcement in combination with the diagonal ties at the joint region is observed to have the highest positive influence on the energy dissipation capacity of joints.

Stiffness degradation

The slope of the straight line joining the peaks of each hysteresis loop represents the secant stiffness for that half cycle. The average stiffness obtained for the two half cycles in a hysteresis loop gives the approximate stiffness for that particular cycle. Figure 11 shows the

stiffness degradation curves of the tested specimens.

Specimens CTRL, SXJ, SXC and SXB

Among these specimens, SXB exhibited the lowest initial stiffness and the fastest stiffness degradation. The initial stiffness values of specimens SXJ and SXC are comparable, but the stiffness degrades rapidly as loading progresses in the case of SXC. The stiffness degradation of specimen SXC is observed to occur at a slower rate compared to the stiffness degradation of specimen CTRL. SXJ exhibited good stiffness properties throughout the loading process than that of the specimen CTRL. This has in effect proved the superiority of the specimen SXJ where diagonal ties have been used as joint transverse reinforcement over the specimen CTRL in promoting the joint stiffness.

Specimens SXJ, SXJ8, SXJ35 and SXJI

The initial stiffness values of these specimens except SXJI are observed to be high with the highest value exhibited by SXJ35. The stiffness property of specimen SXJ8 is found to be superior throughout the loading process. The specimens SXJ and SXJ35 exhibited almost similar stiffness properties during loading. The specimen SXJI exhibited lowest initial stiffness and fastest stiffness degradation unlike the rest of the specimens in this category because of itslower aspect ratio value (0.67). The stiffness property of specimen SXJ can be further enhanced by increasing the area of column longitudinal reinforcement (as in SXJ8).

Reinforcement strain of beam bars

The strains in the beam longitudinal reinforcement are measured at the beam column interface using strain gauges, and they are plotted against the deformations as shown in Figure 12. The mode of failure experienced by each specimen is signified by the strain readings. The specimens failed in beam flexure exhibited the highest reinforcement strains.

Specimens CTRL, SXJ, SXC and SXB

Specimens SXJ and SXC, which failed in the beam flexure mode, exhibited the highest reinforcement strain compared to specimens CTRL and SXB. The strain increased rapidly when the specimens reached the ultimate displacement. The lowest strain is observed in the case of specimen SXB, which experienced shear failure.

Specimens SXJ, SXJ8, SXJ35 and SXJI

Since all these specimens failed in beam flexure, the reinforcement strains are accordingly higher with the highest value shown by the specimen SXJ8. The subsequent higher strains are exhibited by SXJ, SXJ35 and SXJI respectively.

Observations on specimen failure mechanisms

The Figures 7. (a)-(d) represent the failure modes of various specimens. The specimen CTRL is designed with conventional detailing pattern, a characteristic compressive strength of 30 MPa, and unit aspect ratio. The specimen possessed comparatively good joint shear strength and hence failed in beam joint failure mode. The specimen SXB has a design concrete strength of 30 MPa and unit aspect ratio,

Table 4. Strength and deformation characteristics of specimens

Specimen	*CTRL*	*SXB*	*SXC*	*SXJ*	*SXJ35*	*SXJI*	*SXJ8*
Observed shear strength (MPa)	*7.23*	*6.89*	*7.97*	*8.06*	*8.76*	*8.26*	*8.47*
% Change in shear (Comparison with CTRL)	-	*- 5 %*	*+ 10 %*	*+ 11 %*	-	-	-
% Change in shear (Comparison with SXJ)	-	-	-	-	*+ 9 %*	*+ 2 %*	*+ 5 %*
δy (mm)	*20.01*	*25.37*	*17.4*	*17.5*	*16.5*	*28.5*	*16.54*
δu (mm)	*52.31*	*36.78*	*47.12*	*53.9*	*43.73*	*42.15*	*55.10*
Displacement ductility factor	*2.61*	*1.45*	*2.71*	*3.08*	*2.65*	*1.48*	*3.33*
Cumulative energy dissipation (kNm)	*2.48*	*1.32*	*2.62*	*2.74*	*2.54*	*1.35*	*2.83*
Observed mode of failure	*BJF*	*JF*	*BF*	*BF*	*BF*	*BF*	*BF*

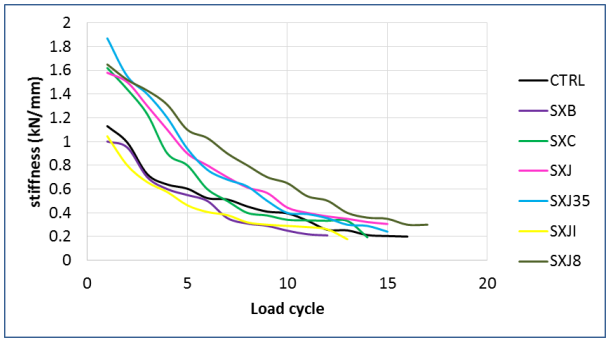

Fig. 11 Stiffness degradation curves

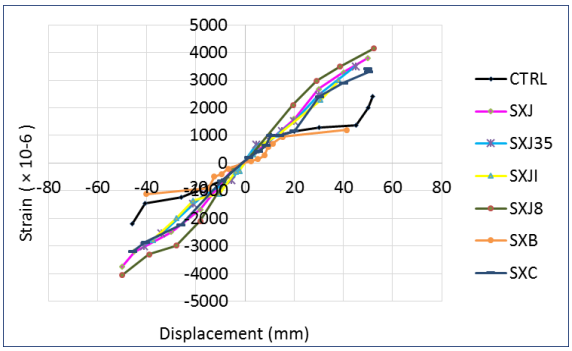

Fig. 12 Reinforcement strain curves

but the detailing pattern consist of X type confining reinforcement placed along the beam direction. This design resulted in poor performance with respect to strength and ductility and ultimately resulted in joint shear failure. In the case of specimen SXC, detailing pattern consist of placing X type confining reinforcement along column direction, and was designed with a concrete characteristic strength of 30 MPa and unit aspect ratio. SXC exhibited very good strength and failed in ductile beam failure mode. The specimens SXJ, SXJ35, SXJ8 and SXJI are designed with cross-inclined stirrups at the joint. All of these specimens experienced beam flexure failure modes. Even though the specimen SXJI exhibited beam failure mode, the failure was almost abrupt with poor ductility properties. This is due to the negative effect the aspect ratio has in the ductile behavior of joints. This has once again emphasized the importance of maintaining unit aspect ratio of joints in possessing sufficient flexibility. The performance of specimens SXJ, SXJ35 and SXJ8 are observed to be superior to the remaining specimens in all respect.

Conclusions

The present experimental investigation indicated that the provision of collar stirrups at the joint is an ideal alternative to the conventional detailing of joint specimens where rectangular stirrups have been in use. The provision of X type confining reinforcement aligned along the column axis is the second-best alternative suggested by the present study. Conclusions drawn from the experimental investigation on joints with proposed reinforcement detailing are given below:

1) The reinforcement detailing consisted of collar stirrups at the joint and X type confining reinforcement aligned along the column axis have supported the ductile beam failure mode, while the reinforcement detailing involving X type confining reinforcement aligned along the beam axis has promoted the brittle shear failure mode.
2) The strength performances in terms of ultimate load and shear strength are observed to enhance significantly in the case of specimens designed with collar stirrups and X type reinforcement aligned along column axis. The highest values are exhibited by the SXJ series specimens indicating the supremacy of collar stirrups over other reinforcement detailing.
3) Specimens detailed with collar stirrups and X type reinforcement aligned along the column have exhibited very good energy dissipation capacity than the conventionally detailed specimen and the specimen with X type reinforcement along the beam axis.
4) The reinforcement detailing consisting of collar stirrups and X type reinforcement aligned along the column axis have promoted the ductility performance of specimens significantly.
5) The ultimate load of specimen designed with collar stirrups has been observed to enhance significantly when the compressive strength was increased from M30 (SXJ) to M35 (SXJ35).
6) The increases in concrete compressive strength and area of column longitudinal bars have been observed to influence the shear strength

positively in the case of specimens designed with collar stirrups at the joint region.

7) The ductile behaviour in terms of displacement ductility and energy dissipation capacity of specimen with collar stirrups is found to be superior when the area of column longitudinal bars was increased significantly.
8) The energy dissipation of specimen with collar stirrups is observed to exhibit more than 50 % depletion in its capacity when the aspect ratio was changed from unity to 0.67.
9) The study recommends the proposed detailing pattern consisting of collar stirrups at the joint region as an excellent alternative to the conventional reinforcement detailing (IS 13920:2016) to be used in beam column joints of moment resisting frames in earthquake prone areas.
10) The provision of X type confining reinforcement aligned along column as transverse reinforcement in joint is recommended as the second-best alternative to the conventional reinforcement detailing to be used in beam column joints of moment resisting frames.

Limitations and future research

The research work on cyclic load performance of RC interior joints has been carried out by giving equal attention to modeling aspects and experimental aspects separately. In establishing the behavior characteristics, the interior joints with main beams only have been considered. The effects of presence of transverse beams, slabs, eccentric beams on shear and ductile behavior of joints need to be investigated. The interior joint properties are established under constant axial loads on the column. The effect of varying axial force in the columns and their influence in the joint behaviour has to be experimentally investigated and quantified.

Acknowledgements

The authors wish to gratefully acknowledge the Government of Kerala (Quality Improvement Programme 2013-2016) for financially supporting this study.

References

1. Abbas, A.A., Mohsin, S.M.S., & Cotsovos, D.M. (2014). Seismic response of steel fibre reinforced concrete beam column joints. *Engineering Structures,* 59, 261–283.
2. Abrams, D.P. (1987). Scale relations for reinforced concrete beam-column joints. *ACI Structural Journal,* 84 (6), 502-512.
3. ACI 318-M14. (2014). *Building code requirements for reinforced concrete and commentary*. American Concrete Institute, Farmington Hills.
4. ACI 352-R02. (2002). *Recommendations for design of beam column connections in monolithic reinforced concrete structures.* American Concrete Institute, Farmington Hills.
5. Alva, G.M.S., De Cresce ElDebs, A.L.H., & El Debs, M.K. (2007). An experimental study on cyclic behaviour of reinforced concrete connections. *Canadian Journal of Civil Engineering,* 34 (4), 565-575. doi: 10.1139/l06-164.
6. Au, F.T.K., Huang, K., & Pam, H.J. (2005). Diagonally reinforced Beam Column joints under cyclic loading. *Structures and Buildings,* 158, 21-40.
7. Bakir, P.G., & Boduroglu, H.M. (2006). Nonlinear analysis of beam column joints using

softened truss model. *Mechanics Research Communications*, 33, 134-147.

8. Bonacci, J., & Pantazopoulou, S. (1993). Parametric investigation of joint mechanics. *ACI Structural Journal*, 90 (1), 61-71.
9. Chalioris, C.E., Favvata, M.J., & Karayannis, E.G. (2008). Reinforced concrete beam–column joints with crossed inclined bars under cyclic deformations. *Earthquake Engineering and Structural Dynamics*, 37, 881-897.
10. Chalioris, C.E., Karayannis, C.G., & Favvata, M.J. (2007). Cyclic testing of reinforced concrete beam column joints with cross inclined bars. In: *Proceedings of the 13th Computational methods and Experimental Measurements (CMEM)*, 623-632. Prague, Czech Republic.
11. Durrani, A.J. & Wight, J.K. (1985). Behaviour of interior beam to column connections under earthquake type loading. *ACI Journal*, 82,343-349.
12. Fu, J., Chen, T., Wang, Z., & Bai, S. (2000). Effect of axial load ratio on seismic behaviour of interior beam column joints. In: *Proceedings of the Twelfth World Conference on Earthquake Engineering*. New-Zealand.
13. Goto, Y., & Joh, O. (1996). An experimental study on shear failure mechanism of reinforced concrete interior beam column joints. In: *Proceedings of the Eleventh World Conference on Earthquake Engineering*,1194. Mexico.
14. IS 1599. (2012). *Metallic Materials-Bend Test*. Bureau of Indian Standards, New Delhi.
15. IS 1786. (2008). *High Strength Deformed Steel Bars and Wires for Concrete Reinforcement*. Bureau of Indian Standards, New Delhi.
16. IS 10262. (2009). *Guidelines for Concrete Mix Design Proportioning*. Bureau of Indian Standards, New Delhi.
17. IS 13920. (2016). *Ductile Detailing of Reinforced Concrete Structures Subjected to Seismic Forces*. Bureau of Indian Standards, New Delhi.
18. Kim, J., & LaFave, J.M. (2008). Probabilistic joint shear strength models for design of RC beam column connections. *ACI Structural Journal*, 105 (6), 770-780.
19. Kitayama, K., Otani, S., & Aoyama, H. (1988). Behaviour of reinforced concrete beam column slab sub assemblages subjected to bi-directional load reversals. In: *Proceedings of the 9th World Conference on Earthquake Engineering*, VIII. Tokyo, Japan.
20. Kitayama, K., Otani, S., & Aoyama, H. (1991). *Development of design criteria for RC interior beam column joints.* ACI SP123-12: Design of Beam Column Joints for Seismic Resistance, 97-123. ACI.
21. Leon, R.T. (1989). Interior joints with variable anchorage lengths. *Journal of Structural Engineering*, 115 (9), 2261-2275.
22. Leon, R.T. (1990). Shear strength and hysteresis behaviour of interior beam column joints. *ACI Structural Journal*, 87 (1), 3-11.
23. Li, L., Mander, J.B., & Dhakal, R.P. (2008). Bidirectional cyclic loading experiment on a 3D beam column joint designed for damage avoidance. *ASCE Journal of Structural Engineering*, 134 (11), 1733-1742.
24. Lu, Y., Vintzileou, E., Zhang, G.F., & Tassios, T.P. (1999). Reinforced concrete scaled columns under cyclic actions. *Soil Dynamics and Earthquake Engineering*, 18, 151-167.

25. Lu, X., Urukap, T.H., Li, S., & Lin, F. (2012). Seismic behaviour of interior RC beam column joints with additional bars under cyclic loading. *Earthquake and Structures,* 3 (1), 37-57.
26. Meinheit, D.F., & Jirsa, J.O. (1977). *The shear strength of reinforced concrete beam column joints.* CESRL Report 77-1, The University of Texas, Austin.
27. Meinheit, D.F., & Jirsa, J.O. (1981). Shear strength of R/C beam column connections. *ASCE Proceedings,* 16668.
28. Mitra, N.S., & Lowes, L.N. (2011). Probabilistic model for failure initiation of reinforced concrete interior beam column connections subjected to seismic loading. *Engineering Structures,* 33, 154-162. doi: 10.1016/j.engstruct.2010.09.029.
29. NZS 3101. (2006). *Concrete structures standard, Part 1: The design of concrete structures*, New Zealand Standard.
30. Pantazopoulou, S. & Bonacci, J. (1992). Consideration of questions about beam column joints. *ACI Structural Journal,* 89 (1), 27-36.
31. Pantazopoulou, S. & Bonacci, J. (1994). On earthquake-resistant reinforced concrete frame connections. *Canadian Journal of Civil Engineering*, 21 (2), 307-328. doi: 10.1139/l94-032.
32. Park, R. & Ruitong. D. (1988). A comparison of the behaviour of reinforced concrete beam column joints designed for ductility and limited ductility. *Bulletin* of the New-Zealand National Society of Earthquake Engineering 21 (4), 255–278.
33. Park, R. & Milburn, J.R. (1998). Comparison of recent New Zealand and United States seismic design provisions for reinforced concrete beam column joints and test results from four units designed according to the New Zealand code. *Bulletin* of the New-Zealand National Society Earthquake Engineering 16 (1), 03-24.
34. Paulay, T., & Priestley, M.J.N. (1992). *Seismic Design of Reinforced Concrete and Masonry Buildings*. New York: John Wiley & Sons.
35. Paulay, T., Park, R., & Priestley, M.J.N. (1978). Reinforced concrete beam column joints under seismic action. *Journal of American Concrete Institute,* **7**5 (11), 585-593.
36. Penelis, G.G., & Kappos, A.J. (2010). *Earthquake Resistant Concrete Structures*. Oxon: Taylor & Francis Group.
37. Shannag, M.J., Abu-Dyya, N., & Abu-Farsakh, G. (2005). Lateral load response of high-performance fibre reinforced concrete beam column joints. *Construction and Building Materials,* 19, 500-508.
38. Shen, X., Li, B., Chen, Y.T., & Tizan, W. (2021). Seismic performance of reinforced concrete interior beam column joints with novel reinforcement detail. *Engineering Structures,* 227, 111408.
39. Shin, M., & LaFave, J.M. (2004). Modelling of cyclic joint shear deformation contributions in RC beam column connections to overall frame behaviour. *Structural Engineering and Mechanics,* 18 (5), 645-669.
40. Shiohara, H. (2004). Quadruple flexural resistance in RC beam column joints. In: *Proceedings of the Thirteenth World Conference on Earthquake Engineering*, 491. Canada.
41. Shiohara, H., & Kusuhara, F. (2009). Comprehensive series of tests on seismic performance of reinforced-concrete beam

column joints. In: *Proceedings of the Third International Conference on Advances in Experimental Structural Engineering*. San-Francisco.

42. Stevens, N.J., Uzumeri, S.M., & Collins, M.P. (1991). Reinforced concrete subjected to reverse cyclic shear-experiments and constitutive model. *ACI Structural Journal,* 88 (2), 135-146.
43. Vandana, R.K., & Bindhu, K.R. (2017). Influence of geometric and material characteristics on the behaviour of reinforced concrete beam column connections. *Canadian Journal of Civil Engineering*, 44, 377–386. *doi:dx.doi.org/10.1139/cjce-2016-0247.*
44. Vandana, R.K., & Bindhu, K.R., & Baiju, K.V. (2018). Probabilistic model for shear strength of RC interior beam column joints. *Journal of Earthquake Engineering*. doi: https://doi.org/10.1080/13632469.2018.1495135.
45. Xing, G.H., Wu, T., Niu, D.T., & Liu, X. (2013). Seismic behaviour of reinforced concrete interior beam column joints with beams of different depths. *Earthquakes and Structures*, 4 (4), 1-000.